Molecular Insight into the Interaction Mechanisms of Amino-2H-Imidazole Derivatives With BACE1 Protease: A QM/MM and QTAIM Study

Esteban Gabriel Vega-Hissi,[a,b] Rodrigo Tosso,[a] Ricardo Daniel Enriz,[a] and Lucas Joel Gutierrez*[c]

In this study, we described quantitatively the interactions between two new amino-2H-imidazole inhibitors ((*R*)-1t and (*S*)-1m) and BACE1 using a hybrid quantum mechanics-molecular mechanical (QM/MM) method together with a quantum theory of atoms In Molecules (QTAIM) analysis. Our computational calculations revealed that the binding affinity of these compounds is mostly related to the amino-2H-imidazole core, which interact tightly with the aspartate dyad of the active site. The interactions were stronger when the inhibitors presented a bulky substituent with a hydrogen bond acceptor motif pointing toward Trp76, such as the 3,5-dimethyl-4-methoxyphenyl group of compound (*S*)-1m. Furthermore, the QTAIM analysis revealed that many hydrophobic interactions complement cooperatively the hydrogen bond which is not present when compound (*R*)-1t is bound to the enzyme. The combined QM/MM-QTAIM analysis allows identifying the interactions that account for the activity difference between compounds, even at a nanomolar range.

DOI: 10.1002/qua.24854

Introduction

Alzheimer's disease (AD), the most common cause of dementia in the elderly, is a devastating ailment that affects millions of people worldwide.[1–3] This neurodegenerative disorder progresses as a general decline in brain function, initially affecting one's cognitive abilities and memories and eventually resulting in incapacitation and death. As the recognition of their central role in APP processing, secretases have been identified as a possible target for therapeutic intervention of AD. α-Secretase has not been targeted because its APP cleavage site is located in the Aβ region and does not lead to the formation of Aβ deposits. However, both β- and γ-secretases have been suggested as targets to inhibit Aβ formation and thereby stop the progression of AD.[4,5]

The first step in the processing of APP to generate Aβ is cleavage by the aspartyl protease β-secretase, or BACE1. This step is followed by γ-secretase cleavage, resulting in Aβ peptides of different lengths. One form of the degradation product, Aβ_{42}, is thought to be particularly pathogenic.[6] Analyzing in detail the pathological mechanism of AD, BACE1 emerges as an attractive molecular target for AD treatment. Regarding this, the development and optimization of BACE1 inhibitors to lower the concentration of Aβ in the brain may prevent or cure AD.

In the last decade, many compounds have been synthesized to inhibit the proteolytic activity of BACE1.[7–9] Recently, Ghosh and Osswald have reported a review about BACE1 inhibitors for the treatment of AD.[10] However, despite extensive research, the identification of a potent BACE1 inhibitor, efficacious in man, has proven to be a challenge.[11–13] Two main structural kinds of BACE1 inhibitors may be found in the bibliography: transition state isosteres of the peptide substrate[14,15] and cyclic structures with an amidine or guanidine moiety, that interacts with the aspartate catalytic dyad of BACE1.[16–20] Two new inhibitors that belong to the cyclic structures group have been recently reported (Fig. 1).[6]

These compounds possess a very interesting pharmacological profile for AD treatment. Among other properties, they have shown: (i) high BACE1 inhibitory activity in an enzymatic assay, (ii) significant BACE1 inhibitory activity in cell assays, (iii) a good cell permeability, and iv) good selectivity versus hERG channel. Moreover, compound (*S*)-1m has produced time-dependent decreases of Aβ_{40} and Aβ_{42} levels in plasma, brain, and CSF in an animal study. Gravenfors et al. have synthesized and cocrystallized these two compounds within the BACE1 active site.[6] These authors have modified the amidine-containing core structure to investigate changes in

[a] *E. G. Vega-Hissi, R. Tosso, R. D. Enriz*
Departamento de Química, Facultad de Química, Bioquímica y Farmacia, and IMIBIO-CONICET, Universidad Nacional de San Luis, Chacabuco 917, (5700) San Luis, Argentina

[b] *E. G. Vega-Hissi*
Área de Química Física, Departamento de Química, Universidad Nacional de San Luis, Chacabuco 917, San Luis, 5700, Argentina

[c] *L. J. Gutierrez*
Laboratorio de Estructura Molecular y Propiedades, Área de Química Física, Departamento de Química, Facultad de Ciencias Exactas y Naturales y Agrimensura, Universidad Nacional del Nordeste, Avda. Libertad 5460, (3400) Corrientes, Argentina
E-mail: lucasgutierrez10@gmail.com

Contract grant sponsor: ANPCyT; contract grant number: PICT 2010-1832 (R.D.E.).
Contract grant sponsor: Universidad Nacional de San Luis (UNSL).
Contract grant sponsor: CONICET by a posdoctoral fellowship (E.G.V.H. and L.J.G.).
Contract grant sponsor: CONICET by a doctoral fellowship (R.T.).

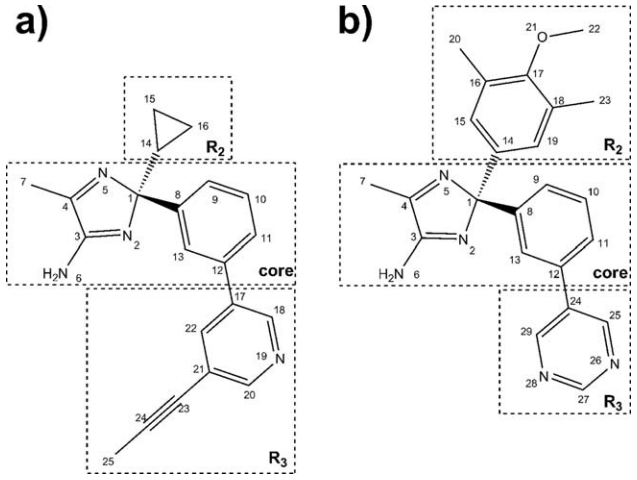

Figure 1. Molecular structure of the two studied amino-2H-imidazole inhibitors. a) Compound *(R)*-1t: R_3: 5-(prop-1-ynyl) pyridin-3-yl; R_2: cyclopropyl. b) Compound *(S)*-1m: R_3: pyrimidin-5-yl; R_2: 3,5-dimethyl-4-methoxyphenyl.

enzyme inhibition and different physicochemical properties related to its biological activity. According to the crystal structure, compounds *(R)*-1t and *(S)*-1m have displayed a similar binding mode within the active site of BACE1. Therefore, it is not possible to explain the stronger inhibitory effect of *(S)*-1m only from the experimental data available. Clearly, the description at molecular level of the different interactions that stabilize and destabilize the formation of both molecular complexes is critical to understand the different biological behavior observed. Furthermore, such information might be useful for the development of new inhibitors with higher potency.

Therefore, to provide a proper description of the intermolecular interactions, it is necessary to consider their nature. In that sense, it is clear that hydrogen bonds are by far the most important specific interactions in biological recognition processes. However, other interactions ranging from strongly electrostatic ones to strongly dispersive ones, such as the dihydrogen bonds, halogen bonds, stacking interactions, dispersion interactions, and X—H $\cdots\pi$ interactions, have been the subject of extensive investigations.[21] As the noncovalent interactions generally are weaker than the covalent ones, it is evident that they are more difficult to be properly described. However, recent advances in computational calculation of the electron charge density have made possible the proper description of the three-dimensional network of bonding and nonbonding interactions in different biological systems[22–26] in the context of the quantum theory of atoms in molecules (QTAIM).[27] Thus, it is now possible to study more accurately the effects of substitutes ligands (bearing small structural modifications) when they interact with their biological receptor.

The main aim of this work is to describe quantitatively the interactions between inhibitors *(R)*-1t and *(S)*-1m and BACE1 from a theoretical point of view. Thus, we have used a hybrid quantum mechanics-molecular mechanical (QM/MM) method in combination with a QTAIM analysis to investigate in detail the binding of this class of inhibitors to the BACE1.

Methods and Computational Details

Molecular model building scheme

The structural models used in this study were obtained from the X-ray crystal structures of the BACE1-*(R)*-1t and BACE1-*(S)*-1m complexes (protein database codes 4B1C and 4B1D, respectively). The missing loops were built by structural superposition between our model and selected crystal coordinates using Chimera software.[28] Residues 158–169 were built from the crystal coordinates of one of the most highly resolved complete structure of BACE1 published so far, protein database code: 1SGZ.[29] Due to the long distance from the recognition surface and its inherent flexibility, the conformations adopted by this loop during our simulations do not influence the binding mode. In agreement with the accepted reaction mechanism for pepsin-like enzymes, the catalytic residues, Asp32 and Asp228, were modeled in a protonated and deprotonated state, respectively.[30–35] Other ionizable groups were assumed as its ionization state at pH 7.0.

Molecular dynamics simulations and MM-GBSA analysis

Molecular dynamics simulations (MD) and subsequent structural analysis were done with the Amber12 package.[36] The all-atom force field ff99SB[37] was used to describe the complexes whereas the waters were represented by the TIP3P model. Each model was soaked in a truncated octahedral periodic box of TIP3P water molecules. The distance between the edges of the water box and the closest atom of the solutes was at least 10 Å. Sodium ions were added to neutralize the charge of the system. The entire system was subjected to energy minimization.

In the next place, each system was then heated in the NVT ensemble from 0 to 300 K in 500 ps and equilibrated at an isothermal isobaric (NPT) ensemble for another 500 ps. A Langevin thermostat[38] was used for temperature coupling with a collision frequency of 1.0 ps^{-1}.The particle mesh Ewald (PME) method was used to treat the long-range electrostatic interactions in a periodic boundary condition.[39] The SHAKE method was used to constrain hydrogen atoms. The time step for all MD is 2 fs, with a direct-space, nonbonded cutoff of 8 Å. Finally, the production was carried out at the NPT ensemble running three independent simulations with length limited to 20 ns, accounting for a total simulation length of 60 ns for each system. The only difference between replicates was the initial velocity assignments at the beginning of the dynamics.

MM-GBSA[40] binding free energy (ΔG_{bind}) resulting from the formation a RL complex between a ligand (L) and a receptor (R) was calculated as:

$$\Delta G_{bind} = \Delta E_{MM} + \Delta G_{sol} - T\Delta S \quad (1)$$

$$\Delta E_{MM} = \Delta E_{internal} + \Delta E_{electrostatic} + \Delta E_{vdw} \quad (2)$$

$$\Delta G_{sol} = \Delta G_{GB} + \Delta G_{SA} \quad (3)$$

where ΔE_{MM}, ΔG_{sol}, and $-T\Delta S$ are the changes of the gas phase MM energy, the solvation free energy, and the

conformational entropy upon binding, respectively. ΔE_{MM} includes $\Delta E_{internal}$ (bond, angle, and dihedral energies), $\Delta E_{electrostatic}$ (electrostatic), and ΔE_{vdw} (van der Waals) energies. ΔG_{solv} is the sum of electrostatic solvation energy (polar contribution), ΔG_{GB}, and the nonelectrostatic solvation component (nonpolar contribution), ΔG_{SA}. Polar contribution is calculated using the GB model, while the nonpolar energy is estimated by solvent accessible surface area (SASA). It should be noted that although the employment of the SASA term gave good results in this work, is under intensive debates and alternative methods to calculate the nonpolar energy contribution can be found in the literature.[41–43] The conformational entropy change $-T\Delta S$ is usually computed by normal-mode analysis, but in this study the entropy contributions were not calculated due to the computational cost involved in such calculations.

QM/MM analysis

Partitioning strategy and ONIOM setup. A two-layer ONIOM (QM/MM) method has been used.[44] The compounds, *(R)*-1t or *(S)*-1m, and the side chains of the residues that have at least one heavy atom within 4 Å from the ligand molecule (first shell residues) were incorporated into the high-level QM layer. The chosen cutoff value has resulted from a compromise between computational cost and efficiency, as has been discussed elsewhere.[45,46] Moreover, the partitioning scheme used was designed to obtain an appropriate low-value in the substituent value test (*S*-value).[44] The remainder of the system was incorporated into the low-level MM layer. Only the geometry of the QM layer was fully optimized. Computations were carried out at the ONIOM (B3LYP/6-31G(d):Amber)EE and ONIOM (B3LYP-D/6-31G(d):Amber)EE levels,[47–50] where EE represents the electronic embedding scheme. Electronic embedding incorporates the partial charges of the MM layer into the quantum mechanical Hamiltonian, providing a better description of the electrostatic interaction between the QM and MM layers (as it is treated at the QM level) and allowing the QM wavefunction to be polarized.[44] The MM parameters absent in the standard AMBER force field[51] were included from the generalized amber force field (GAFF).[52]

Quantum mechanics binding energy calculations. The binding energy ($\Delta E_{binding}$) between the inhibitor and the binding site residues (QM layer including backbone atoms of the binding site residues) of both, BACE1-*(R)*-1t and BACE1-*(S)*-1m complexes, was computed as single-point energy calculations at the B3LYP/6-31G(d) and B3LYP-D/6-31G(d) levels of theory, according to the following equation:[53]

$$\Delta E_{binding} = E_{complex} - E_{inh} - E_{BindingSite} + BSSE \quad (4)$$

where $E_{complex}$, E_{inh}, and $E_{BindingSite}$ are the energies of the inhibitor bound to the binding site residues, the isolated inhibitor, and the residues of the binding site, respectively. The BSSE term accounts for the basis set superposition error corrections.[54,55] The geometries of both systems were obtained from the ONIOM optimization. All of these calculations were carried out with Gaussian 09 suite of programs.[56]

Atoms in molecules theory

The wave functions of the inhibitors bound to the binding site residues (QM layer including backbone atoms of the binding site residues), generated at the B3LYP-D/6-31G(d) level of theory, were subjected to a QTAIM analysis[27] using Multiwfn software.[57] This type of calculations have been used in recent works because it ensures a reasonable compromise between the wave function quality required to obtain reliable values of the derivatives of $\rho_{(r)}$ and the computer power available, due to the extension of the system in study (423 and 430 atoms of BACE1-*(R)*-1t and BACE1-*(S)*-1m complexes, respectively).[22,23,25]

Results and Discussions

Validation of the optimized structures and binding energies

The agreement of the structures obtained from the QM/MM geometric optimizations for the complexes (R)-1t/BACE 1 and (S)-1m/BACE1 with their respective crystal structures reported by Gravenfors et al.[6] was evaluated through a superimposition analysis.

Figure 2 clearly shows that the optimization process leads to subtle changes in the orientation and position of the two inhibitors regarding the crystal structures. The differences between the ONIOM (B3LYP/6-31G(d):Amber)EE optimized and experimental structures (including all atoms) have been quantized as the root-mean-square deviations (RMSD) using the program Chimera, with values of 0.121 and 0.137 Å for the complexes of compounds *(R)*-1t and *(S)*-1m, respectively. The RMSD values of the geometries optimized taking into account Grimme's dispersion correction[50] yielded values of 0.581 and 0.653 Å for the complexes of compounds *(R)*-1t and *(S)*-1m, respectively.

The binding energies of compounds *(R)*-1t and *(S)*-1m bound to BACE1 active site were calculated by using three different approaches: MM-GBSA, B3LYP/6-31G(d), and B3LYP-D/6-31G(d). The binding energy gaps obtained for the inhibitors were: 3.27, 9.00, and 19.27 kcal/mol from MM-GBSA, B3LYP/6-31G(d), and B3LYP-D/6-31G(d), respectively. These results indicate that compound *(S)*-1m can bind to the protease more strongly than *(R)*-1t. Although the three approaches used here are qualitatively in agreement with the experimental results, B3LYP-D/6-31G(d) displayed the highest binding energy gap. Thus, it is encouraging that the ranking of the experimental binding energies is consistent with our theoretical calculations which suggest that the structures obtained from the ONIOM scheme are reliable. Therefore, the RMSD values along with the binding energy analysis indicate that the ONIOM optimization scheme generates adequate structures to be used as starting point for a more accurate theoretical analysis. The incorporation of Grimme's dispersion correction[50] leads to a more proper description of the binding affinity between these inhibitors and BACE1 and therefore B3LYP-D/6-31G(d) calculations were used in the rest of the study.

It should be noted that the IC_{50} values obtained from experimental data are very close, and it is very difficult to explain

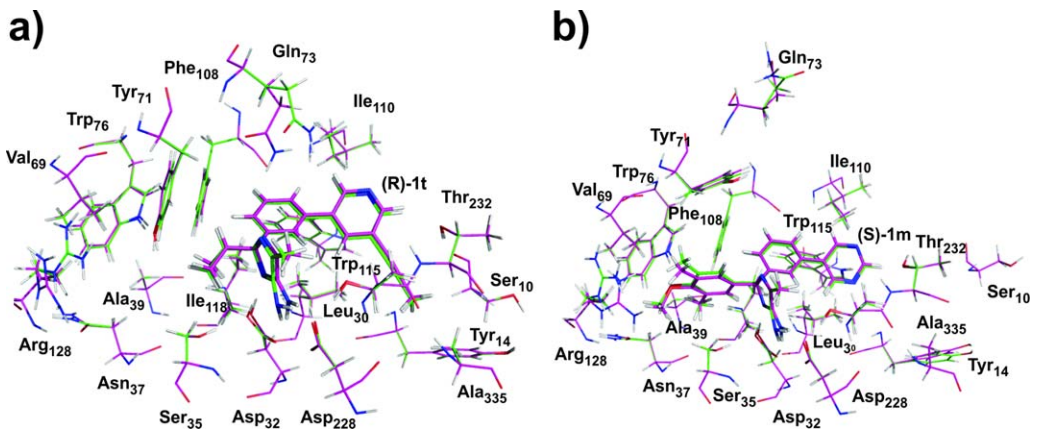

Figure 2. Spatial superimposition of the inhibitors interacting with the active site of BACE1. a) BACE1-*(R)*-1t complex and b) BACE1-*(S)*-1m complex. The X-ray structure is shown in green sticks and the QM/MM (B3LYP-D/6-31G(d)) optimized structure is shown in purple sticks.

the cause of such small differences in activity through standard theoretical calculations.[23] In fact, the analysis based only on the crystallographic structures leads to think that the higher activity of *(S)*-1m is only due to a hydrogen bond interaction with Trp76.[6] However, it is clear that such small differences might be explained only from a more exhaustive electronic density analysis of both complexes. There are many works discussing this interesting problem in the literature. Our own studies have demonstrated the importance to include QTAIM analysis to solve these intricacies.[22,23,25,26] Thus, in the next step of our study we performed a QTAIM study of these complexes using B3LYP-D/6-31G(d) calculations.

Analysis to the binding contribution of the different substituents of (S)-1m and (R)-1t

To acquire a quantitative and more detailed insight into the binding mechanism of compounds *(R)*-1t and *(S)*-1m to BACE1, the interactions were analyzed by QTAIM theory at the B3LYP-D/6-31G(d) level of theory. Figure 3 suggests that the interaction spectra of the two inhibitors with BACE1 are closely related and reflects that their binding modes are similar. It can be also seen that the sum of the intermolecular interactions $\rho_{(r)}$ values is higher in BACE1-(*S*)-1m complex (0.4315 a.u.) than in the BACE1-*(R)*-1t complex (0.4045 a.u.), which indicates that the enzyme presents more affinity for the inhibitor *(S)*-1m.

As can be clearly seen in Figure 3, the core fragment of both compounds presents the highest binding affinity to the enzyme and the strongest interactions that involve the residues Asp32 and Asp228. These amino acids play a key role in the proteolytic activity, and both have been previously reported as important anchoring residues in the interaction of BACE1 with potent inhibitors.[58] The amino-2H-imidazole ring of the core presents four hydrogen bond interactions correctly oriented in terms of the length and angle ($N2_{(R)\text{-}1t/(S)\text{-}1m}\cdots HD2_{Asp32}$, $H32_{(R)\text{-}1t/(S)\text{-}1m}\cdots OD2_{Asp228}$, $H62_{(R)\text{-}1t/(S)\text{-}1m}\cdots OD1_{Asp32}$, $N6_{(R)\text{-}1t/(S)\text{-}1m}\cdots OD1_{Asp228}$, Fig. 4), which represent approximately the 38% and 44% of the sum of $\rho_{(r)}$ intermolecular interactions

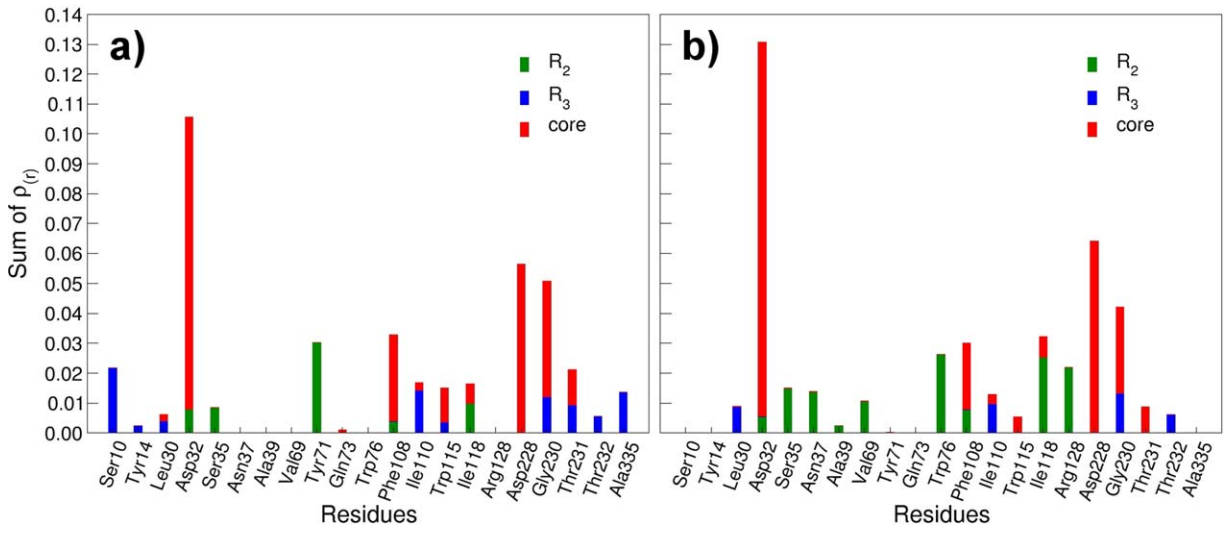

Figure 3. Sum of the values of charge density ($\sum\rho_{(r)}$) at the bond critical points (considering only the intermolecular interactions) in a) BACE1-*(R)*-1t and b) BACE1-*(S)*-1m. These values were partitioned into three contributions: interactions involving residues of the R_2 fragment (green); involving residues of the R_3 fragment (blue); and interactions involving the region of core (red).

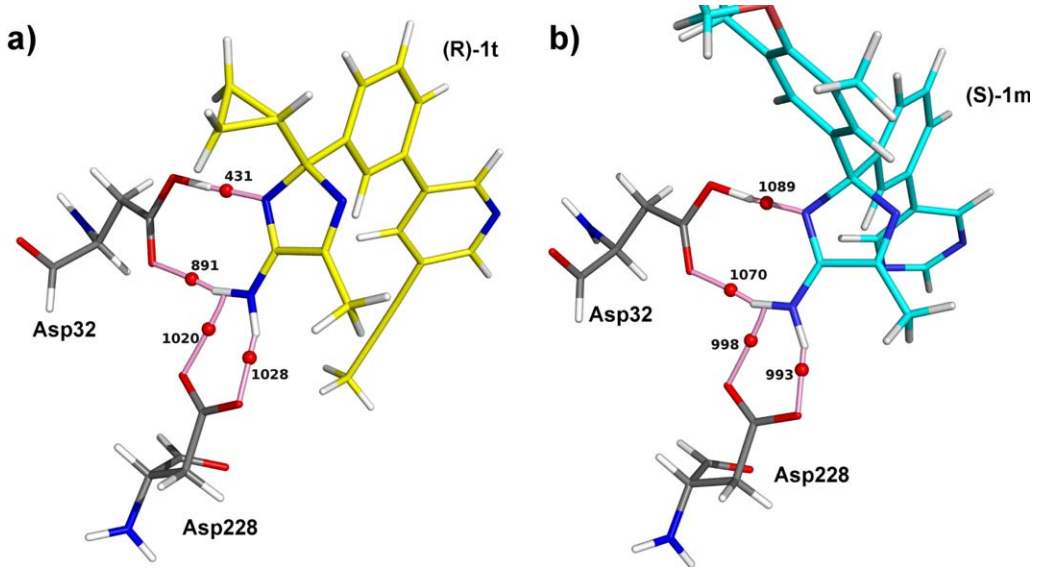

Figure 4. Molecular graph of the noncovalent interactions between the key catalytic residues (Asp32 and Asp228) of BACE1 with a) *(R)*-1t (yellow sticks) and b) *(S)*-1m (cyan sticks). The elements of the electron density topology are shown. The bond paths connecting the nuclei are represented in pink sticks and the bond critical points are shown as red spheres. Additional information of each bond critical point can be found in Tables S1 and S2 of Supporting Information.

values of the complexes of compounds *(R)*-1t and *(S)*-1m, respectively. In addition, these high values of $\rho_{(r)}$ might be indicative of a charge transfer H-bond. These results indicate that the inhibitory potency of these compounds is mostly related to the core-1 region, which agrees with the experimental information.[6]

Another residue located at the catalytic site of BACE1 interacting with the core of these inhibitors is Gly230, which acts as both H-acceptor ($H13_{(R)\text{-}1t/(S)\text{-}1m}\cdots O_{Gly230}$ and $H73_{(S)\text{-}1m}\cdots O_{Gly230}$) and H-donor ($N6_{(R)\text{-}1t/(S)\text{-}1m}\cdots HA3_{Gly230}$; Fig. 5). Interestingly, these H-bonds have also been reported for other inhibitors of BACE1.[59–61] In addition, Gly230 presents a weak O···N interaction ($N6_{(R)\text{-}1t/(S)\text{-}1m}\cdots O_{Gly230}$).

The edge-to-face (T-shaped) configuration of the aromatic rings of the amino acids Phe108, Trp231 and the core phenyl moiety of both inhibitors allows the formation of multiple hydrophobic attractive contacts: $C11_{(R)\text{-}1t/(S)\text{-}1m}\cdots HH2_{Trp115}$, $H11_{(R)\text{-}1t}\cdots HZ2_{Trp115}$, $H10_{(R)\text{-}1t/(S)\text{-}1m}\cdots CD1_{Phe108}$, $H9_{(R)\text{-}1t}\cdots HE1_{Phe108}$ (Fig. 6). The common interaction motif of the latter residues toward these inhibitors has also been previously reported in other compounds such as 5-substituted isophthalamides[59,62] and AZD3839.[63] Moreover, Phe108 establishes a hydrogen bond with the phenyl group of *(R)*-1t ($H10_{(R)\text{-}1t}\cdots O_{Phe108}$) and two hydrogen bonds with the same group of *(S)*-1m ($H10_{(S)\text{-}1m}\cdots O_{Phe108}$ and $H11_{(S)\text{-}1m}\cdots O_{Phe108}$).

Despite these important contacts, the inhibitors are further stabilized by establishing interactions with other residues of the active site wall. The specific contacts depend on the orientation of the different substituents of the aminoimidazole core toward the different subpockets of BACE1.[64,65] The R_2 substituent of both inhibitors lies within the S2'sp subpocket and several differences in the binding mode might be observed in Figures 7a

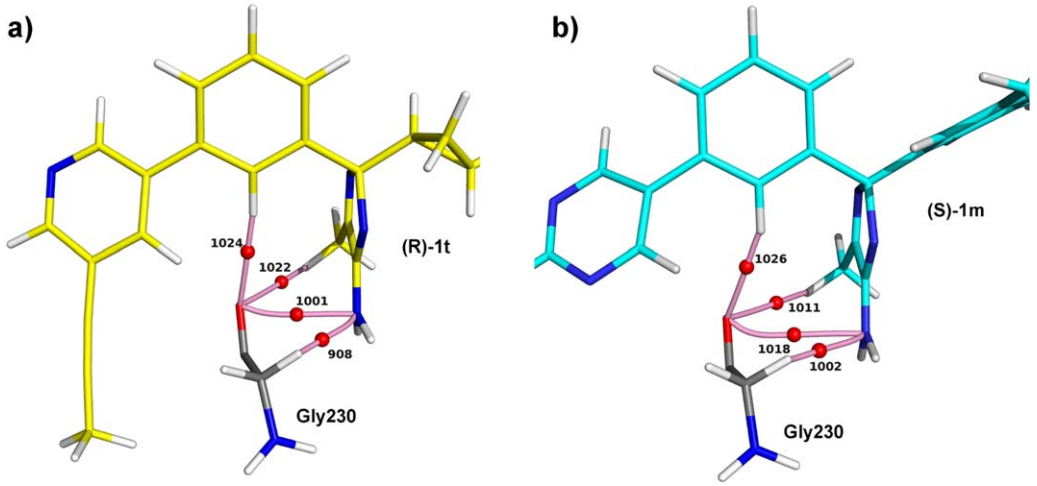

Figure 5. Molecular graph showing the noncovalent interactions between the residue Gly230 of BACE1 with a) *(R)*-1t and b) *(S)*-1m.

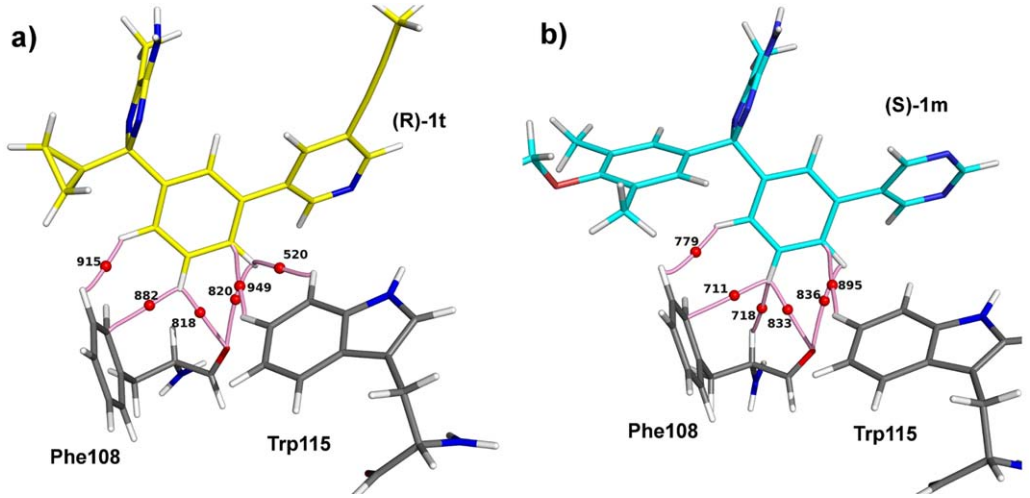

Figure 6. Molecular graph of the noncovalent interactions between residues Phe108 and Trp115 of BACE1 with *(R)*-1t (a) and *(S)*-1m (b).

and 7b. The 3,5-dimethyl-4-methoxyphenyl group (substituent R_2 in *(S)*-1m) makes more favorable interactions than the cyclopropyl group (R_2 group of *(R)*-1t), and therefore, binds tighter to BACE1. This might explain, at least in part, the higher inhibitory activity of *(S)*-1m with respect to *(R)*-1t.[6]

The cyclopropyl group of compound *(R)*-1t is mainly involved in hydrophobic interactions with Tyr71 as has been proposed in the crystal structure according to the distance between these groups (Fig. 7a).[6] Moreover, as can be seen in this figure, there are two weak hydrogen bond interactions of the type CH···O between R_2 and the amino acids Tyr71 and Asp32 ($H161_{(R)\text{-}1t}\cdots OH_{Tyr71}$ and $H162_{(R)\text{-}1t}\cdots OD2_{Asp32}$, respectively) that stabilize the complex. The small size of this substituent allows the surrounding residues of the protein to adopt a proper orientation to establish an intramolecular hydrogen bond between Trp76 and Tyr71, as was previously reported.[6]

On the contrary, many contacts comprising the residues Ser35, Asn37, Ala39, Val69, Trp76, Phe108, Ile118, and Arg128 stabilize the bulky 3,5-dimethyl-4-methoxyphenyl group of compound *(S)*-1m. These interactions are tabulated in Table S2 of Supporting Information. The most prominent one is the moderate hydrogen bond interaction with Trp76 ($O21_{(S)\text{-}1m}\cdots HE1_{Trp76}$, 0.0145 $\rho_{(r)}$ a.u.), which is thought to be responsible for its high potency and is missing in the complex of compound *(R)*-1t (compare Figs. 7a and 7b).[6,66] However, it should be considered that the remaining hydrophobic interactions must complement the hydrogen bond in a cooperative way. In fact, groups like R_2 of compound *(S)*-1m, capable of hydrogen bonding with Trp76 (along with the cooperation of multiple hydrophobic interactions) have been previously used in the design of new and potent inhibitors.[63,67]

Regarding the R_3 substituents of compounds *(R)*-1t and *(S)*-1m, both posses a common portion that is involved in hydrophobic interactions with the same residues (Ile110, Leu30, and Gly230) of the S1 and S3 subpockets of BACE1. However, the alkyl moiety, only present in *(R)*-1t, extends deeply into the S3

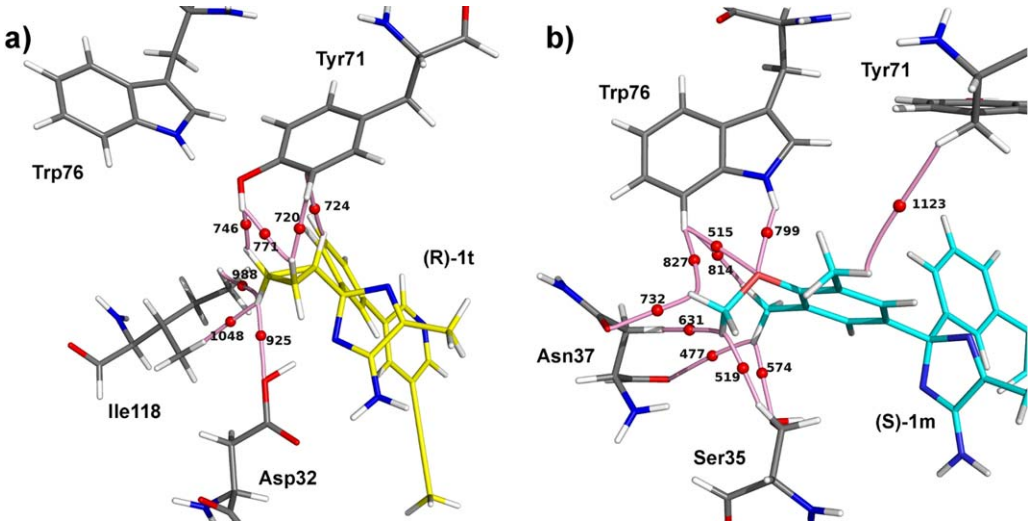

Figure 7. Molecular graph of the noncovalent interactions between the R_2 substituent of a) *(R)*-1t and b) *(S)*-1m with the SP2′ subpocket of BACE1. The remainder interactions are tabulated in Tables S1 and S2 of Supporting Information.

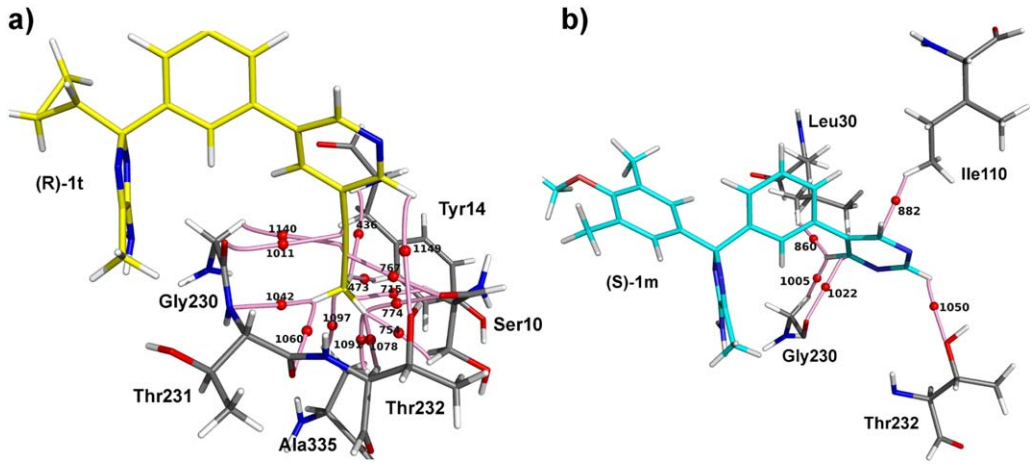

Figure 8. Molecular graph of the noncovalent interactions between the R_3 substituent of a) *(R)*-1t and b) *(S)*-1m with the S3 subpocket of BACE1. For clarity, only most prominent interactions are shown.

subpocket (S3sp), making multiple favorable contacts with Ser10, Gly230, Thr231, Thr232, and Ala335 (Fig. 8, Supporting Information Tables S1 and S2). It should be noted that the overall value of $\rho_{(r)}$ is 0.0622 a.u., which enhances the binding affinity of this inhibitor to this subpocket. Although the R_3 substituent of compound *(R)*-1t confers additional stability, its lipophilic chemical nature improves the chance of increased undesirable effect on the hERG channel.[6,67]

In contrast, the small pyrimidin-5-yl group (R_3 substituent of *(S)*-1m), which reaches only the entrance of the S3sp, is involved in a few weak interactions (Leu30, Ile110, Gly230, and Thr232, the sum of $\rho_{(r)}$ is 0.0378 a.u.) and do not provide further stabilization (Fig. 8, Supporting Information Tables S1 and S2).

Conclusions

BACE1 continues to be an attractive drug design target for the treatment of AD. Unfortunately the emergence of an effective BACE1 inhibitor drug has not yet materialized due to a number of challenging issues. BACE1 inhibitors need to have access to the CNS compartment because this molecular target is located in the brain. Therefore, inhibitors are required to have low molecular weight and other characteristics to achieve effective blood–brain-barrier penetration. In addition, inhibitors need to have high selectivity over other aspartic acid proteases such as BACE2 and cathepsin D, which show high active site homology with BACE1.

The results obtained in this study allowed us to draw interesting conclusions about two different aspects. On the one hand, we evaluated in detail the different molecular interactions that stabilize and destabilize the formation of the enzyme-inhibitor complexes. This led to a better understanding of the different behavior of these two inhibitors of BACE1. This is interesting from the point of view of medicinal chemistry, particularly considering the contributions that can be made about a possible pharmacophoric pattern for these ligands. To design new inhibitors of BACE1 is very useful to understand the molecular aspects governing enzyme–ligand interactions.

Conversely, these results are also interesting from the methodological point of view as they show that from relatively simple molecular modeling techniques it is possible to explain the behavior of two inhibitors with a similar affinity for the enzyme. In this sense, it is important to point out the accuracy of the combined QM/MM-QTAIM analysis that identifies the interactions accounting for the activity difference between compounds, even at a nanomolar range. It should be noted that the inclusion of Grimme's dispersion correction is important when dispersion interactions account for the activity difference between ligands.

Our computational calculations, performed at the molecular level of two amino-2H-imidazoles, revealed that the core is the largest fragment responsible for the inhibitory activity, supporting the conclusion of Ginman et al., who suggested that the core is the region that needs to be early optimized in the lead generation phase to define a framework for future modifications.[67] The activity difference between these two compounds is mainly due to the different contribution of the R_2 group to the binding affinity. The interactions of the inhibitors within S2'sp are stronger when the R_2 substituent is bulky and presents a hydrogen bond acceptor motif pointing toward Trp76, such as the 3,5-dimethyl-4-methoxyphenyl group of compound *(S)*-1m. Furthermore, the QTAIM analysis allowed us to identify that the preference of BACE1 toward *(S)*-1m is due to hydrophobic interactions with residues Asn37, Val69, Ile118, and Arg128 which complement cooperatively the hydrogen bond that is missing in the *(R)*-1t complex. Although the R_3 group confers certain additional stability, especially for BACE1-*(R)*-1t, the introduction of a more lipophilic substituent (more permeable) becomes a compromise between permeability and hERG affinity.

It is important to be cautious with this type of study as while these techniques have been used with good performance in other biological systems, the approach used in this work is only suitable for this type of biological systems. However, we consider our results useful for the interactions analysis and to provide details on the structure–affinity relationship

of these complexes for the pharmacophoric discernment and development of new inhibitors. Addressing the cause of the affinity difference between known drugs might lead to define the essential interactions that need to be present for the future development of new more potent inhibitors.

Acknowledgment

R.D.E. is member of the Consejo Nacional de Investigaciones Científicas y Técnicas (CONICET-Argentina) staff.

Keywords: Alzheimer's disease · BACE1 · molecular modeling: QM/MM calculations · QTAIM

How to cite this article: E. G., Vega-Hissi, R. Tosso, R. D. Enriz, L. J. Gutierrez *Int. J. Quantum Chem.* **2014**, DOI: 10.1002/qua.24854

Additional Supporting Information may be found in the online version of this article.

[1] J. Hardy, D. J. Selkoe, *Science* **2002**, *297*, 353.
[2] D. J. Selkoe, *Science* **1997**, *275*, 630.
[3] R. E. Olson, R. A. Copeland, D. Seiffert, *Curr. Opin. Drug Discov. Devel.* **2001**, *4*, 390.
[4] R. Vassar, *J. Mol. Neurosci.* **2001**, *17*, 157.
[5] R. Vassar, D. M. Kovacs, R. Yan, P. C. Wong, *J. Neurosci.* **2009**, *29*, 12787.
[6] Y. Gravenfors, J. Viklund, J. Blid, T. Ginman, S. Karlstro, J. Kihlstro, K. Kolmodin, J. Lindstro, S. Von Berg, F. Von Kieseritzky, C. Slivo, B. Swahn, L. Olsson, P. Johansson, S. Eketja, J. Fälting, F. Jeppsson, K. Strömberg, J. Janson, F. Rahm, *J. Med. Chem.* **2012**, *55*, 9297.
[7] H. Rueeger, R. Lueoend, O. Rogel, J.-M. Rondeau, H. Möbitz, R. Machauer, L. Jacobson, M. Staufenbiel, S. Desrayaud, U. Neumann, *J. Med. Chem.* **2012**, *55*, 3364.
[8] M. M. Weiss, T. Williamson, S. Babu-Khan, M. D. Bartberger, J. Brown, K. Chen, Y. Cheng, M. Citron, M. D. Croghan, T. A. Dineen, J. Esmay, R. F. Graceffa, S. S. Harried, D. Hickman, S. A. Hitchcock, D. B. Horne, H. Huang, R. Imbeah-Ampiah, T. Judd, M. R. Kaller, C. R. Kreiman, D. S. La, V. Li, P. Lopez, S. Louie, H. Monenschein, T. T. Nguyen, L. D. Pennington, C. Rattan, T. San Miguel, E. A. Sickmier, R. C. Wahl, P. H. Wen, S. Wood, Q. Xue, B. H. Yang, V. F. Patel, W. Zhong, *J. Med. Chem.* **2012**, *55*, 9009.
[9] Y. Cheng, T. C. Judd, M. D. Bartberger, J. Brown, K. Chen, R. T. Fremeau, D. Hickman, S. A. Hitchcock, B. Jordan, V. Li, P. Lopez, S. W. Louie, Y. Luo, K. Michelsen, T. Nixey, T. S. Powers, C. Rattan, E. A. Sickmier, D. J. St Jean, R. C. Wahl, P. H. Wen, S. Wood, *J. Med. Chem.* **2011**, *54*, 5836.
[10] A. K. Ghosh, H. L. Osswald, *Chem. Soc. Rev.* **2014**, *43*, 6765.
[11] J. S. Albert, *Prog. Med. Chem.* **2009**, *48*, 133.
[12] G. Evin, G. Lessene, S. Wilkins, *Recent Pat. CNS Drug Discov.* **2011**, *6*, 91.
[13] G. Probst, Y. Xu, *Expert Opin. Ther. Pat.* **2012**, *22*, 511.
[14] A. K. Ghosh, D. Shin, G. Koelsch, X. Lin, J. Ermolieff, J. Tang, *J. Am. Chem. Soc.* **2000**, *122*, 3522.
[15] J. N. Cumming, U. Iserloh, M. E. Kennedy, *Curr. Opin. Drug Discov. Devel.* **2004**, *7*, 536.
[16] M. S. Malamas, J. Erdei, I. Gunawan, J. Turner, Y. Hu, E. Wagner, K. Fan, R. Chopra, A. Olland, J. Bard, S. Jacobsen, R. L. Magolda, M. Pangalos, A. J. Robichaud, *J. Med. Chem.* **2010**, *53*, 1146.
[17] G. Tresadern, F. Delgado, O. Delgado, H. Gijsen, G. J. Macdonald, D. Moechars, F. Rombouts, R. Alexander, J. Spurlino, M. Van Gool, J. A. Vega, A. A. Trabanco, *Bioorg. Med. Chem. Lett.* **2011**, *21*, 7255.
[18] B.-M. Swahn, J. Holenz, J. Kihlström, K. Kolmodin, J. Lindström, N. Plobeck, D. Rotticci, F. Sehgelmeble, M. Sundström, S. von Berg, J. Fälting, B. Georgievska, S. Gustavsson, J. Neelissen, M. Ek, L.-L. Olsson, S. Berg, *Bioorg. Med. Chem. Lett.* **2012**, *22*, 1854.
[19] P. C. May, R. A. Dean, S. L. Lowe, F. Martenyi, S. M. Sheehan, L. N. Boggs, S. A. Monk, B. M. Mathes, D. J. Mergott, B. M. Watson, S. L. Stout, D. E. Timm, E. Smith Labell, C. R. Gonzales, M. Nakano, S. S. Jhee, M. Yen, L. Ereshefsky, T. D. Lindstrom, D. O. Calligaro, P. J. Cocke, D. Greg Hall, S. Friedrich, M. Citron, J. E. Audia, *J. Neurosci.* **2011**, *31*, 16507.
[20] J. N. Cumming, E. M. Smith, L. Wang, J. Misiaszek, J. Durkin, J. Pan, U. Iserloh, Y. Wu, Z. Zhu, C. Strickland, J. Voigt, X. Chen, M. E. Kennedy, R. Kuvelkar, L. A. Hyde, K. Cox, L. Favreau, M. F. Czarniecki, W. J. Greenlee, B. A. McKittrick, E. M. Parker, A. W. Stamford, *Bioorg. Med. Chem. Lett.* **2012**, *22*, 2444.
[21] C. F. Matta and R. J. E. Boyd, The Quantum Theory of Atoms in Molecules. From solid State to DNA and Drug Design; Wiley-VCH, Weinheim, **2007**.
[22] S. A. Andujar, R. D. Tosso, F. D. Suvire, E. Angelina, N. Peruchena, N. Cabedo, D. Cortes, R. D. Enriz, *J. Chem. Inf. Model.* **2012**, *52*, 99.
[23] R. D. Tosso, S. A. Andujar, L. Gutierrez, E. Angelina, R. Rodríguez, M. Nogueras, H. Baldoni, F. D. Suvire, J. Cobo, R. D. Enriz, *J. Chem. Inf. Model.* **2013**, *53*, 2018.
[24] S. Andujar, F. Suvire, I. Berenguer, N. Cabedo, P. Marín, L. Moreno, M. Dolores Ivorra, D. Cortes, R. D. Enriz, *J. Mol. Model.* **2012**, *18*, 419.
[25] J. Párraga, N. Cabedo, S. Andujar, L. Piqueras, L. Moreno, A. Galán, E. Angelina, R. D. Enriz, M. D. Ivorra, M. J. Sanz, D. Cortes, *Eur. J. Med. Chem.* **2013**, *68*, 150.
[26] E. L. Angelina, S. A. Andujar, R. D. Tosso, R. D. Enriz, N. M. Peruchena, *J. Phys. Org. Chem.* **2014**, *27*, 128.
[27] R. F. W. Bader, *Acc. Chem. Res.* **1985**, *18*, 9.
[28] E. F. Pettersen, T. D. Goddard, C. C. Huang, G. S. Couch, D. M. Greenblatt, E. C. Meng, T. E. Ferrin, *J. Comput. Chem.* **2004**, *25*, 1605.
[29] L. Hong, J. Tang, *Biochemistry* **2004**, *43*, 4689.
[30] D. R. Davies, *Annu. Rev. Biophys. Biophys. Chem.* **1990**, *19*, 189.
[31] K. Suguna, E. A. Padlan, C. W. Smith, W. D. Carlson, D. R. Davies, *Proc. Natl. Acad. Sci. USA* **1987**, *84*, 7009.
[32] A. Barman, R. Prabhakar, *J. Mol. Graph. Model.* **2013**, *40*, 1.
[33] H. Park, S. Lee, *J. Am. Chem. Soc.* **2003**, *125*, 16416.
[34] A. A. Gorfe, A. Caflisch, *Structure* **2005**, *13*, 1487.
[35] A. Barman, R. Prabhakar, *J. Chem. Inf. Model.* **2012**, *52*, 1275.
[36] D. A. Case, T. E. Cheatham, T. Darden, H. Gohlke, R. Luo, K. M. Merz, A. Onufriev, C. Simmerling, B. Wang, R. J. Woods, *J. Comput. Chem.* **2005**, *26*, 1668.
[37] K. Lindorff-Larsen, S. Piana, K. Palmo, P. Maragakis, J. L. Klepeis, R. O. Dror, D. E. Shaw, *Proteins* **2010**, *78*, 1950.
[38] J. A. Izaguirre, D. P. Catarello, J. M. Wozniak, R. D. Skeel, *J. Chem. Phys.* **2001**, *114*, 2090.
[39] U. Essmann, L. Perera, M. L. Berkowitz, T. Darden, H. Lee, L. G. Pedersen, *J. Chem. Phys.* **1995**, *103*, 8577.
[40] A. Onufriev, D. Bashford, D. A. Case, *J. Phys. Chem. B* **2000**, *104*, 3712.
[41] P. Kar, M. Seel, U. H. E. Hansmann, S. Höfinger, *J. Phys. Chem. B* **2007**, *111*, 8910.
[42] S. Höfinger, F. Zerbetto, *Chem. Phys. Lett.* **2009**, *480*, 313.
[43] P. Kar, M. Seel, T. Weidemann, S. Höfinger, *FEBS Lett.* **2009**, *583*, 1909.
[44] T. Vreven, K. S. Byun, I. Komáromi, S. Dapprich, J. A. Montgomery, K. Morokuma, M. J. Frisch, *J. Chem. Theory Comput.* **2006**, *2*, 815.
[45] X. Guo, D. He, L. Huang, L. Liu, L. Liu, H. Yang, *Comput. Theor. Chem.* **2012**, *995*, 17.
[46] X. Guo, D. He, L. Liu, R. Kuang, L. Liu, *Comput. Theor. Chem.* **2012**, *991*, 134.
[47] A. D. Becke, *J. Chem. Phys.* **1993**, *98*, 5648.
[48] C. Lee, W. Yang, R. G. Parr, *Phys. Rev. B* **1988**, *37*, 785.
[49] W. J. Hehre, R. Ditchfield, J. A. Pople, *J. Chem. Phys.* **1972**, *56*, 2257.
[50] S. Grimme, *J. Comput. Chem.* **2006**, *27*, 1787.
[51] W. D. Cornell, P. Cieplak, C. I. Bayly, I. R. Gould, K. M. Merz, D. M. Ferguson, D. C. Spellmeyer, T. Fox, J. W. Caldwell, P. A. Kollman, *J. Am. Chem. Soc.* **1995**, *117*, 5179.
[52] J. Wang, R. M. Wolf, J. W. Caldwell, P. A. Kollman, D. A. Case, *J. Comput. Chem.* **2004**, *25*, 1157.
[53] S. Saen-oon, M. Kuno, S. Hannongbua, *Proteins* **2005**, *61*, 859.
[54] S. F. Boys, F. Bernardi, *Mol. Phys.* **1970**, *19*, 553.
[55] S. Simon, M. Duran, J. J. Dannenberg, *J. Chem. Phys.* **1996**, *105*, 11024.
[56] M. J. Frisch, G. W. Trucks, H. B. Schlegel, G. E. Scuseria, M. A. Robb, J. R. Cheeseman, G. Scalmani, V. Barone, B. Mennucci, G. A. Petersson, H. Nakatsuji, M. Caricato, X. Li, H. P. Hratchian, A. F. Izmaylov, J. Bloino, G. Zheng, J. L. Sonnenberg, M. Hada, M. Ehara, K. Toyota, R. Fukuda, J.

Hasegawa, M. Ishida, T. Nakajima, Y. Honda, O. Kitao, H. Nakai, T. Vreven, J. A. Montgomery Jr., J. E. Peralta, F. Ogliaro, M. Bearpark, J. J. Heyd, E. Brothers, K. N. Kudin, V. N. Staroverov, R. Kobayashi, J. Normand, K. Raghavachari, A. Rendell, J. C. Burant, S. S. Iyengar, J. Tomasi, M. Cossi, N. Rega, J. M. Millam, M. Klene, J. E. Knox, J. B. Cross, V. Bakken, C. Adamo, J. Jaramillo, R. Gomperts, R. E. Stratmann, O. Yazyev, A. J. Austin, R. Cammi, C. Pomelli, J. W. Ochterski, R. L. Martin, K. Morokuma, V. G. Zakrzewski, G. A. Voth, P. Salvador, J. J. Dannenberg, S. Dapprich, A. D. Daniels, Ö. Farkas, J. B. Foresman, J. V Ortiz, J. Cioslowski, D. J. Fox, "Gaussian 09."*; Gaussian Inc., Pittsburg,* **2009**.

[57] T. Lu, F. Chen, *J. Comput. Chem.* **2012**, *33*, 580.

[58] N. S. Andreeva, L. D. Rumsh, *Protein Sci.* **2001**, *10*, 2439.

[59] N. Razzaghi-Asl, A. Ebadi, N. Edraki, S. Shahabipour, and R. Miri, *Med. Chem. Res.* **2012**, *22*, 3259.

[60] J. Madden, J. R. Dod, R. Godemann, J. Kraemer, M. Smith, M. Biniszkiewicz, D. J. Hallett, J. Barker, J. D. Dyekjaer, T. Hesterkamp, *Bioorg. Med. Chem. Lett.* **2010**, *20*, 5329.

[61] C. A. Coburn, S. J. Stachel, K. G. Jones, T. G. Steele, D. M. Rush, J. DiMuzio, B. L. Pietrak, M.-T. Lai, Q. Huang, J. Lineberger, L. Jin, S. Munshi, M. Katharine Holloway, A. Espeseth, A. Simon, D. Hazuda, S. L. Graham, J. P. Vacca, *Bioorg. Med. Chem. Lett.* **2006**, *16*, 3635.

[62] S. J. Stachel, C. A. Coburn, T. G. Steele, M.C. Crouthamel, B. L. Pietrak, M.T. Lai, M. K. Holloway, S. K. Munshi, S. L. Graham, J. P. Vacca, *Bioorg. Med. Chem. Lett.* **2006**, *16*, 641.

[63] F. Jeppsson, S. Eketjäll, J. Janson, S. Karlström, S. Gustavsson, L.L. Olsson, A.C. Radesäter, B. Ploeger, G. Cebers, K. Kolmodin, B.M. Swahn, S. von Berg, T. Bueters, J. Fälting, *J. Biol. Chem.* **2012**, *287*, 41245.

[64] L. Hong, G. Koelsch, X. Lin, S. Wu, S. Terzyan, A. K. Ghosh, X. C. Zhang, J. Tang, *Science.* **2000**, *290*, 150.

[65] R. T. Turner, L. Hong, G. Koelsch, A. K. Ghosh, J. Tang, *Biochemistry* **2005**, *44*, 105.

[66] B. Swahn, K. Kolmodin, S. Karlstro, S. Von Berg, P. Söderman, J. Holenz, S. Berg, J. Lindström, M. Sundström, D. Turek, J. Kihlström, C. Slivo, L. Andersson, D. Pyring, D. Rotticci, Ö. Liselotte, A. Kers, K. Bogar, F. Von Kieseritzky, M. Bergh, L. Olsson, J. Janson, S. Eketjäll, B. Georgievska, F. Jeppsson, J. Fälting, *J. Med. Chem.* **2012**, *55*, 9346.

[67] T. Ginman, J. Viklund, J. Malmström, J. Blid, R. Emond, R. Forsblom, A. Johansson, A. Kers, F. Lake, F. Sehgelmeble, K. J. Sterky, M. Bergh, A. Lindgren, P. Johansson, F. Jeppsson, J. Fälting, Y. Gravenfors, F. Rahm, *J. Med. Chem.* **2013**, *56*, 4181.

Received: 29 July 2014
Revised: 26 November 2014
Accepted: 9 December 2014
Published online on Wiley Online Library